Stress response of a clinical Enterococcus faecalis isolate subjected to a novel antimicrobial surface coating

Clauss-Lendzian, Emanuel; Vaishampayan, Ankita; de Jong, Anne; Landau, Uwe; Meyer, Carsten; Kok, Jan; Grohmann, Elisabeth

Published in:
Microbiological Research

DOI:
10.1016/j.micres.2017.11.006

Publication date:
2018

Microbiological Research 207 (2018) 53–64

Contents lists available at ScienceDirect

Microbiological Research

journal homepage: www.elsevier.com/locate/micres

Stress response of a clinical *Enterococcus faecalis* isolate subjected to a novel antimicrobial surface coating

Emanuel Clauss-Lendzian[a], Ankita Vaishampayan[b], Anne de Jong[c], Uwe Landau[d], Carsten Meyer[d], Jan Kok[c], Elisabeth Grohmann[a,b,*]

[a] Division of Infectious Diseases, University Medical Center Freiburg, Hugstetter Straße 55, 79106 Freiburg im Breisgau, Baden-Württemberg, Germany
[b] School of Life Sciences and Technology, Beuth University of Applied Sciences, Seestrasse 64, 13347 Berlin, Germany
[c] Department of Molecular Genetics, University of Groningen, Nijenborgh 7, 9747 Groningen, The Netherlands
[d] Largentec GmbH, Am Waldhaus 32, 14129 Berlin, Germany

ARTICLE INFO

Keywords:
Antimicrobial
Silver
Stress
RNA sequencing
Enterococcus

ABSTRACT

Emerging antibiotic resistance among pathogenic bacteria, paired with their ability to form biofilms on medical and technical devices, represents a serious problem for effective and long-term decontamination in health-care environments and gives rise to an urgent need for new antimicrobial materials. Here we present the impact of AGXX®, a novel broad-spectrum antimicrobial surface coating consisting of micro-galvanic elements formed by silver and ruthenium, on the transcriptome of *Enterococcus faecalis*. A clinical *E. faecalis* isolate was subjected to metal stress by growing it for different periods in presence of the antimicrobial coating or silver-coated steel meshes. Subsequently, total RNA was isolated and next-generation RNA sequencing was performed to analyze variations in gene expression in presence of the antimicrobial materials with focus on known stress genes. Exposure to the antimicrobial coating had a large impact on the transcriptome of *E. faecalis*. After 24 min almost 1/5 of the *E. faecalis* genome displayed differential expression. At each time-point the *cop* operon was strongly up-regulated, providing indirect evidence for the presence of free Ag^+-ions. Moreover, exposure to the antimicrobial coating induced a broad general stress response in *E. faecalis*. Genes coding for the chaperones GroEL and GroES and the Clp proteases, ClpE and ClpB, were among the top up-regulated heat shock genes. Differential expression of thioredoxin, superoxide dismutase and glutathione synthetase genes indicates a high level of oxidative stress. We postulate a mechanism of action where the combination of Ag^+-ions and reactive oxygen species generated by AGXX® results in a synergistic antimicrobial effect, superior to that of conventional silver coatings.

1. Introduction

Enterococci are Gram-positive bacteria with a two-sided nature. As harmless commensals they are present in the gastrointestinal tract of animals ranging from insects to humans (Gilmore et al., 2014). However, Enterococci are also known as opportunistic nosocomial pathogens that can cause endocarditis, sepsis and wound as well as urinary tract infections (Theilacker et al., 2012). Actually, *Enterococcus* species are the second most common pathogens in healthcare-associated infections; among enterococcal hospital-acquired infections approx. 60% are assigned to *E. faecalis* (Hidron et al., 2008). This species is able to form biofilms on medical devices such as catheters and orthopedic implants (Mohamed and Huang, 2007). In these biofilms the bacteria are protected from a variety of physical as well as chemical stresses making them hard to eradicate and thus medically important (Costerton et al., 1999; Lewis, 2001). Moreover, Enterococci are naturally resistant to many antibiotics and able to acquire and exchange antibiotic resistance determinants giving them a selective advantage in environments with heavy antibiotic usage such as hospitals (Gilmore et al., 2014). An infamous example is *E. faecalis* V583, the first clinical isolate resistant to vancomycin (Sahm and Olsen, 1990).

Silver was the most important antimicrobial compound before antibiotics were introduced in the 1940s (Alexander, 2009; Mijnendonckx et al., 2013). Since ancient times, silver and copper have been used for medical applications. Silver is receiving renewed attention as antimicrobial surface material and is becoming increasingly prevalent in clinics and general healthcare (Lansdown, 2006) as a broad-spectrum agent with activity against Gram-positive and Gram-negative bacteria, fungi, protozoa and certain viruses but low toxicity to human cells (Maillard and Hartemann, 2012; Mijnendonckx et al., 2013). The most

* Corresponding author at: School of Life Sciences and Technology, Beuth University of Applied Sciences, Seestrasse 64, 13347 Berlin, Germany.
E-mail address: elisabeth.grohmann@beuth-hochschule.de (E. Grohmann).

https://doi.org/10.1016/j.micres.2017.11.006
Received 20 May 2016; Received in revised form 21 April 2017; Accepted 7 November 2017
Available online 12 November 2017
0944-5013/

prominent forms are silver ions (mostly as $AgNO_3$) and silver nanoparticles (Prabhu and Poulose, 2012). However, extensive use of silver has raised questions and concerns about its safety and toxicity for the human body and the environment, as well as the risk associated with the reported increase in microbial resistance (Lansdown, 2010; Maillard and Hartemann, 2012; Mijnendonckx et al., 2013). Biofilm production, in combination with the huge problem of emerging antibiotic resistance among clinically relevant bacteria, gives rise to an urgent need for new antimicrobial materials. One of these is AGXX®, a novel broad-spectrum antimicrobial surface coating (Guridi et al., 2015) consisting of silver (Ag) and ruthenium (Ru) conditioned with ascorbic acid. The antimicrobial surface coating can be electroplated homogenously on various carrier materials such as steel, glass, ceramics and organic polymers like polydimethylsiloxane. In contrast to conventional silver nanotechnology, the electroplating process results in a surface structured by micro-galvanic elements of Ag and Ru. The antimicrobial coating is durable, recyclable and thus environmentally friendly. It has already been successfully applied in industrial water disinfection (Landau, 2013).

Although the mechanism of antimicrobial action of copper and silver is not yet fully understood, it is known that free bioavailable ions of these metals and the generation of reactive oxygen species (ROS) such as the highly reactive hydroxyl radicals (OH·) play important roles. Cu^+- and Ag^+-ions are isovalent electronic and have the same d^{10} electron configuration. Moreover, they show a similar protein coordination chemistry (Loftin et al., 2007). Therefore, it is not surprising that some proteins can bind and transport both metal ions, e.g. the *E. coli* binding protein CusF (Kittleson et al., 2006) and the exporter CusCBA encoded by the *cus* (Cu *s*ensitivity) operon (Franke et al., 2003). Silver ions interact with thiol groups of proteins, block respiration and electron transfer and promote the production of ROS (Gordon et al., 2010; Park et al., 2009). Upon excess of intracellular copper, an important trace element and cofactor for many indispensable enzymes, hydroxyl radicals can be generated in a Fenton-type reaction (Grass et al., 2011) that participate in the oxidation of proteins, lipids and DNA (Imlay, 2003; Yoshida et al., 1993). Therefore, metal ion homeostasis plays a critical role in the defense against oxidative stress and is even key to successful host colonization, infection and survival (Agranoff and Krishna, 1998), making it an important modulator of bacterial pathogenicity (Abrantes et al., 2013, 2011; Wang et al., 2014). The best understood prokaryotic metal homeostasis system is specified by the extensively studied *cop* operon of *E. hirae*. It regulates the uptake, availability and export of copper (Odermatt and Solioz, 1995; Odermatt et al., 1994, 1993; Solioz and Stoyanov, 2003; Wunderli-Ye and Solioz, 1999). The *cop* operon is inducible by Cu^{2+}, Cd^{2+} and Ag^+ (Odermatt et al., 1993) and consists of four genes: *copY* codes for a copper-responsive repressor, *copZ* encodes a copper chaperone/transport protein, and *copA* and *copB* specify copper transporting ATPases (Solioz and Stoyanov, 2003).

The evolution of specific and adaptive responses is crucial for survival in habitats with varying conditions. Stress response pathways, such as the heat shock and SOS response pathways, as well as the response to oxidative stress, are widely conserved and exhibit regulatory connections (Derré et al., 1999; Layton and Foster, 2003; Neher et al., 2006). Upon exposure to various stress conditions such as heat shock, but also during chemical and oxidative stresses, a signaling pathway known as the heat shock response is turned on; it is characterized by a markedly increased expression of genes coding for molecular chaperones and Clp proteases (Hartl et al., 2011; Mattoo and Goloubinoff, 2014). Mis- or unfolded proteins and polypeptide chains are assisted in (re-) folding to their native conformation by these chaperones (Hartl et al., 2011) or degraded by the Clp proteases (Neher et al., 2006) to prevent their aggregation. Oxidative stress can be generated by oxygen and various ROS, such as hydrogen peroxide (H_2O_2) and hydroxyl radicals (OH·). ROS can cause serious damage to nucleic acids, proteins and lipids via oxidation (Imlay, 2003), which may ultimately lead to cell death (Gordon et al., 2010). They are usually inactivated quickly by protective enzymes such as superoxide dismutase and catalase. The thioredoxin system and glutaredoxins keep proteins in their reduced state (Arnér and Holmgren, 2000) and are therefore important additional players in the response to oxidative stress. DNA damage or the collapse of DNA replication forks as a consequence of ROS results in the exposure of vulnerable single stranded DNA, inducing the bacterial SOS response (Lusetti and Cox, 2002; Michel, 2005). It generally consists of the induction of genes coding for DNA repair proteins such as exonucleases, helicases and recombinases as well as translesion DNA polymerases (van der Veen and Abee, 2011) and is primarily regulated by the repressor LexA (Butala et al., 2009) and the activator RecA (Cox, 2007). All these conserved rescue pathways enable bacteria to tolerate and survive various forms of stress.

In this study, we subjected the clinical *E. faecalis* 12030 isolate to metal stress by exposing it to AGXX® or Ag-coated V2A steel meshes, examined the transcriptome responses by next-generation RNA sequencing and analyzed variations in gene expression to elucidate the mechanism of action of the antimicrobial AGXX® at the molecular level.

2. Material and methods

2.1. Preparation and testing of antimicrobial metal meshes

The metal meshes were essentially prepared as previously described (Guridi et al., 2015). Stainless steel gauze (V2A: DIN ISO 1.4301), 50 µm mesh width, was used as base material for Ag and AGXX® coatings as well as reference material. The silver and AGXX® coatings were electroplated on the stainless steel carrier meshes with the same thickness of 3–5 µm. The resulting AGXX® coating is structured such that many micro-galvanic cells are formed on the surface layer consisting of Ag micro anodes and Ru micro cathodes. The antimicrobial activity of AGXX® meshes was routinely checked by incubation with *Escherichia coli* DSM 498 at 37 °C for 18 h.

2.2. Media and growth conditions

E. faecalis 12030 (Huebner et al., 1999) was grown at 37 °C in Brain Heart Infusion (BHI, Oxoid Deutschland GmbH, Wesel, Germany) medium with constant agitation at 150 rpm or on BHI agar (Oxoid Deutschland GmbH). For generation of growth curves, bacteria were pre-cultured overnight, diluted in BHI medium to an optical density at 600 nm (OD_{600}) of 0.05 and incubated for 8 h either in the presence of an uncoated V2A mesh (abbreviated as V2A) or a V2A mesh coated with AGXX® (AGXX®) or silver (Ag) (12 cm^2 each in 30 ml medium to obtain a mesh-surface to medium-volume ratio of 0.4); cultures grown in the absence of a metal mesh served as controls. The OD_{600} of the cultures was measured using a Genesys™ 10 UV–vis spectrophotometer (Thermo Spectronic, Rochester, USA). Colony Forming Units (CFU) ml^{-1} were determined hourly from 0 to 8 h post inoculation. Growth experiments were performed in triplicate with independent biological replicates.

2.3. Metal stress and RNA isolation

Overnight cultures of *E. faecalis* 12030 were diluted as described above and grown until mid-exponential growth phase ($OD_{600} \approx 0.6$). The cultures were then either subjected to metal stress by exposure to an AGXX®- or Ag-coated metal mesh or exposed to an uncoated V2A steel mesh (mesh-surface to medium-volume ratio of 0.4) followed by further incubation for 3, 6, 12, 24, 60 and 90 min at 37 °C with constant agitation of 150 rpm. As a control, no metal mesh was added.

Cells from 30 ml culture were harvested by centrifugation for 1 min at 10 000 rpm and 4 °C in a Sorvall RC6+ centrifuge (Thermo Scientific GmbH, Langenselbold, Germany). Cell pellets were immediately frozen in liquid nitrogen and stored at −80 °C or directly used for RNA

isolation. RNA was isolated using the ZR Fungal/Bacterial RNA MiniPrep™Kit (Zymo Research, Freiburg, Germany) following the manufacturer's instructions. To recover total RNA including small RNAs, 1.5 vols of absolute ethanol were added in step 5. Finally, total RNA was eluted with 50 µl DNase-/RNase-free water and stored at −80 °C. RNA quantity and quality were assessed with Agilent RNA 6000 Nano and Pico Kits using an Agilent 2100 Bioanalyzer (Agilent Technologies, Santa Clara, USA). Residual contaminating DNA was digested with DNA-*free*™ DNase (Ambion, Carlsbad, USA).

2.4. RNA sequencing and data analysis

To remove rRNAs and tRNAs from the total RNA, MICROB*Express*™ and MEGAclear™ Kits were applied. After purification, 500 ng of the enriched (m)RNA was fragmented with RNase III. Fragmented (m)RNA (50–100 ng) was used for the preparation of barcoded whole transcriptome cDNA libraries using the Ion Total RNA-Seq Kit v2 and Ion Xpress™ RNA-Seq Barcode 1–16 Kits. Finally, strand-specific, multiplexed RNA sequencing was carried out on Ion PI™ chips in an Ion Proton™ Sequencer by PrimBio (Exton, PA, USA). All kits and devices for RNA sequencing were from Ambion, Carlsbad, USA and were used according to the manufacturer's instructions.

Raw sequencing reads were aligned to the reference genome of *E. faecalis* 12030 using Bowtie2 (Langmead and Salzberg, 2012) version 2.2.3. Post-processing of the SAM files into sorted BAM files was performed with SAMtools (Li et al., 2009 version 1.2–207). Length-normalized confidence interval FPKM (=Fragments Per Kilobase of exon per Million fragments mapped) values were obtained with Cufflinks (Trapnell et al., 2010) using optimized settings for the Ion Proton™ Sequencer. Finally, statistical analysis was carried out with the recently developed T-REx RNA sequencing expression analysis pipeline (de Jong et al., 2015) using the differential expression method of EdgeR (Robinson et al., 2010). A gene was considered significantly differentially expressed when the expression ratio was $\geq|2.0|$ and the false discovery rate (FDR) adjusted p-value ≤ 0.05. The data presented in this work have been deposited in NCBI's Gene Expression Omnibus (Edgar et al., 2002) and are accessible through GEO Series accession number GSE79250 (https://www.ncbi.nlm.nih.gov/geo/query/acc.cgi?acc=GSE79250).

2.5. Reverse transcription quantitative PCR (RT-qPCR) and data analysis

To investigate if gene expression in *E. faecalis* 12030 is influenced by Ag or AGXX®, RT-qPCR was performed as a second independent method. To this end, RNA from *E. faecalis* 12030 cultures subjected to Ag or AGXX® for 0 (control) or 24 min was extracted as described in 'Metal stress and RNA isolation'. First strand cDNA was synthesized with RevertAid™ First Strand cDNA Synthesis kit (Thermo Fisher Scientific Inc., Walham, Germany) as per the manufacturer's instructions using 200 ng total RNA as template and random hexamer primers. cDNA was diluted with DNase/RNase-free water and amplified in a LightCycler®480 II (Roche Diagnostics GmbH, Mannheim, Germany). The *copY*, *copZ*, *groES*, *sodA* and *gap* genes were amplified using TaqMan chemistry according to the instructions and protocol provided in LightCycler®480 Probes Master Kit (Roche Diagnostics). All RT-qPCRs were carried out in a total volume of 20 µl. The amplification step was performed with 'Quantification' analysis mode at 95 °C for 10 s, with a ramp rate of 4.4 °C/second, followed by annealing at the respective annealing temperature for 50 s, with a ramp rate of 2.2 °C/s and finally an extension at 72 °C for 1 s, with a ramp rate of 4.4 °C/s. The amplification step was performed 45 times.

All primers and probes used in the study are listed in Table A.3 in the Supplementary Information. All RT-qPCR experiments were performed in triplicate and each experiment was repeated at least twice. Data was analyzed by LightCycler® 480 Software release 1.5.0 by using the Livak method for relative quantification (Livak and Schmittgen, 2001). The *E. faecalis gap* gene was used as a reference (Aakra et al., 2005; Aakra et al., 2010). Data represent fold changes in gene expression, calculated by normalizing to *gap* and relative to the Calibrator (culture without antimicrobial material). Means of four Cp values each were used to calculate the fold change in gene expression. Fold change and standard deviation are plotted.

2.6. Statistical analysis

Statistical tests were performed to analyze the significance of the obtained data. Student's *t*-test was applied to the delta Cp values. The tests were performed and analyzed using SigmaPlot version 11.0 (Systat software, Inc., San Jose California USA, www.systatsoftware.com).

2.7. Detection of hydrogen peroxide

Photometric detection of H_2O_2 is based on the oxidation of Fe^{2+} to Fe^{3+} and subsequent red complex formation of Fe^{3+} with xylenol orange (Gupta, 1973). The xylenol orange dye solution was prepared of 0.025 mM xylenol orange disodium salt, 0.2 mM ammonium iron(II) sulfate hexahydrate and 2.5 mM sulfuric acid. Extinction at 585 nm was measured with a Specord® 50 UV/Vis-spectrophotometer (Analytik Jena AG, Jena, Germany). A calibration curve was generated using H_2O_2 solutions in concentrations from 2 to 10 µM. The exact H_2O_2 concentration was determined by titration with 0.2 M potassium permanganate solution. All chemicals were obtained from Sigma-Aldrich Chemie GmbH (Schnelldorf, Germany).

Experiments in separated half-cells were performed with a 1 cm^2 sheet of 99.9% Ag (MaTecK GmbH, Juelich, Germany) and 99.9% Ru (MaTecK GmbH), respectively, in glass vials filled with 4 ml xylenol orange dye solution, connected by a salt bridge consisting of a teflon tube (inner diameter 0.25 mm) filled with the same solution. The cell voltage between Ag and Ru was measured using mixtures of potassium chloride and potassium nitrate (both from Sigma-Aldrich Chemie GmbH) with a total ionic strength of 1 M, therefrom 0 to 1 M potassium chloride.

3. Results

3.1. AGXX® has a strong antimicrobial effect

While AGXX® is active against a large number of Gram-positive and Gram-negative bacteria (Guridi et al., 2015) it exhibits only slight cytotoxicity on a human lung fibroblast cell line (Bouchard, 2011). We investigated the transcriptional response of *E. faecalis* 12030 to metal stress induced by antimicrobial Ag and AGXX® coatings using next-generation RNA sequencing technology to elucidate the mode of action of AGXX® at the level of gene expression. By challenging *E. faecalis* 12030 with these antimicrobial coatings for different short (several min) and long (up to 1.5 h) exposure times we covered both a possible quick and transient stress response as well as a potential adaptation reaction. To simplify, we will refer to this exposure to Ag or AGXX® coatings as "metal stress". The whole transcriptome response of *E. faecalis* 12030 grown in the presence of an Ag- or AGXX®-coated metal mesh was compared to that of *E. faecalis* 12030 grown without any metal mesh.

To prove that the chosen mesh-surface to medium-volume ratio of 0.4 had an inhibitory effect, growth experiments were performed in batch cultures, determining the colony forming units (CFU) ml^{-1} at hourly intervals with different metal mesh types (Fig. 1).

CFU ml^{-1} values of *E. faecalis* 12030 grown in the presence of V2A and Ag were not significantly different from those of control cultures that were not exposed to a metal mesh. This was expected for non-antimicrobial V2A, but not for antimicrobial Ag. In contrast, a very strong inhibitory effect was observed for *E. faecalis* 12030 incubated with AGXX® (Fig. 1): Already one hour after inoculation, the CFU ml^{-1} value was less than one

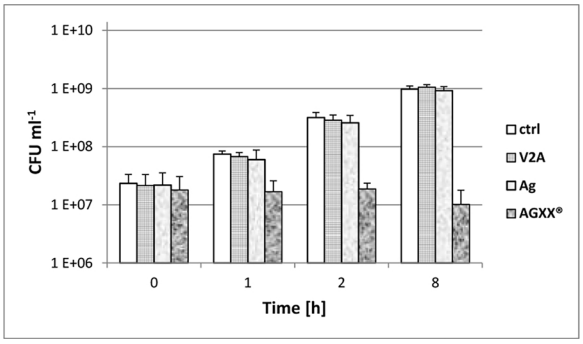

Fig. 1. AGXX®-mediated growth inhibition of *E. faecalis* 12030 in batch culture. CFU ml^{-1} values are plotted against the time in h post inoculation with log10 scale. Control cultures (ctrl) were grown without any metal mesh. V2A: uncoated, stainless steel mesh; Ag: silver-coated V2A mesh; AGXX®: AGXX®-coated V2A mesh. Time-point 1 represents early exponential, time-point 2 mid-exponential and time-point 8 stationary growth phase. Mean values are given (n = 3) and error bars denote the standard deviation.

fourth of that of the control cultures ($1.68 \times 10^7 \pm 9.08 \times 10^6$ in comparison to $7.45 \times 10^7 \pm 9.57 \times 10^6$). After 8 h of incubation, the CFU ml^{-1} value ($1.02 \times 10^7 \pm 7.72 \times 10^6$) was diminished to approx. 57% of the initial inoculation CFU ml^{-1} value ($1.80 \times 10^7 \pm 1.26 \times 10^7$) (Fig. 1). This is evidence not only for growth inhibition but for killing of *E. faecalis* 12030 by AGXX®.

3.2. AGXX® has a huge impact on the transcriptome of E. faecalis

RNA sequencing showed that exposure to the antimicrobial AGXX® had an enormous impact on the transcriptome of *E. faecalis* 12030 in terms of differential gene expression. Table 1 presents an overview of the total number of up- and down-regulated genes at each time-point versus controls (at time-point 0 min, in each case after growth until mid-exponential growth phase; this is applied throughout the whole study).

Whenever the exposure time was doubled starting from time-point 3 min until time-point 24 min, the total number of differentially expressed genes also approximately doubled. Of all exposure times, 24 min had the largest impact on the transcriptome of *E. faecalis* 12030. At that time-point almost one fifth of all of the genes of *E. faecalis* 12030 were differentially expressed and the largest difference (i.e. strongest anti-correlation) in gene expression compared to the controls was observed (Fig. 2).

3.3. Gene expression in E. faecalis exposed for 24 min to V2A, Ag and AGXX®

A Venn diagram (Fig. 3) was created to determine the common and unique genes that were differentially expressed in *E. faecalis* 12030 exposed to the three different metal mesh types. This was done for the 24 min samples as this exposure time to AGXX® (after growth until mid-exponential growth phase) resulted in the largest total number of differentially expressed genes (Table 1) and the largest difference in gene expression (Fig. 2) in *E. faecalis* 12030.

Subsequently, a gene set enrichment analysis (GSEA) was performed on Clusters of Orthologous Groups (COG) categories (Tatusov et al., 2000) of the genes for which such COG categories are defined, in order to determine which COG categories were most affected by the various metal mesh types.

Table 1
Number of differentially expressed genes in *E. faecalis* 12030 exposed to AGXX® versus controls.

	3 min	6 min	12 min	24 min	60 min	90 min
Up-regulated genes	46	114	242	373	185	242
Down-regulated genes	15	29	110	227	44	222
Total number	61	143	352	600	229	464
% of the genome	2.0	4.7	11.5	19.5	7.5	15.1

The percentage of the genome affected by AGXX® was calculated as quotient of the total number of differentially expressed genes relative to the control samples and the number of protein encoding genes of *E. faecalis* 12030 (3073) (Aziz et al., 2008) × 100.

3.4. COG categories of common differentially expressed genes

More than one fourth of all 348 common differentially expressed genes in *E. faecalis* 12030 exposed to AGXX®, Ag or V2A (Fig. 3) were members of the COG category "Carbohydrate transport and metabolism". Other overrepresented COG categories were "Translation, ribosomal structure and biogenesis" (approx. 15% of the 348 common differentially expressed genes), "Amino acid transport and metabolism" and "Energy production and conversion" (both 8%). The two most significantly overrepresented COG categories were "Cell wall/membrane/envelope biogenesis" (approx. 1.5%) and "Replication, recombination and repair" (approx. 3%).

The GSEA of the 26 genes that were common between *E. faecalis* 12030 grown with AGXX® or Ag (Fig. 3) but were not differentially expressed in the presence of V2A, showed that the COG "Inorganic ion transport and metabolism" was significantly affected (approx. 21% of the 26 common differentially expressed genes). Two of these genes, namely *EF.peg.3039* (peg: protein encoding gene) and *EF.peg.3040*, are part of the *cop* operon. The *cop* operon of *E. hirae* regulates the uptake, availability and export of copper in this organism (Solioz and Stoyanov, 2003). Furthermore, the third gene of the *cop* operon, *EF.peg.3041* encoding the CopY repressor, was also up-regulated in *E. faecalis* 12030 exposed for 24 min to either AGXX® or Ag. Their individual fold changes, however, were much higher in *E. faecalis* 12030 exposed to AGXX® (Table 2) than in cells exposed to Ag (Table A1 in the Supplementary information).

139 genes respond to the presence of AGXX® or V2A but not to Ag (Fig. 3). The three most significantly overrepresented COG categories among these genes were "Inorganic ion transport and metabolism" (approx. 10%; genes of the *cop* operon are not part of this group), "Translation, ribosomal structure and biogenesis" (approx. 9%) and "Lipid transport and metabolism" (approx. 8%).

3.5. COG categories of unique differentially expressed genes

The most prevalent and moreover top overrepresented COG category among the 177 unique differentially expressed genes in *E. faecalis* 12030 exposed to V2A was "Translation, ribosomal structure and biogenesis" (approx. 18% of the 177 genes). Approximately 11%, 10% and 7% belong to the COG categories "Transcription", "Cell wall/membrane/envelope biogenesis" and "Lipid transport and metabolism", respectively.

In *E. faecalis* 12030 grown in the presence of Ag the predominant COG category of the 70 unique differentially expressed genes was "Carbohydrate transport and metabolism" (approx. 16% of the 70 genes) followed by "Amino acid transport and metabolism" and "Transcription" (approx. 13% each). Other overrepresented COG categories were "Energy production and conversion", "Coenzyme transport and metabolism" as well as "Signal transduction mechanisms".

For the most interesting sample – *E. faecalis* 12030 exposed for 24 min, the exposure time resulting in the largest total number of differentially expressed genes and the largest difference in gene expression observed for antimicrobial AGXX® – we distinguished between up and down-regulation in the GSEA of the 87 unique differentially expressed genes. The most prevalent and moreover top overrepresented COG category of the 35 up-regulated genes was "Inorganic ion transport and metabolism" (approx. 17%). All three genes encoding a zinc uptake system homologous to the zinc uptake system ZnuABC first described in

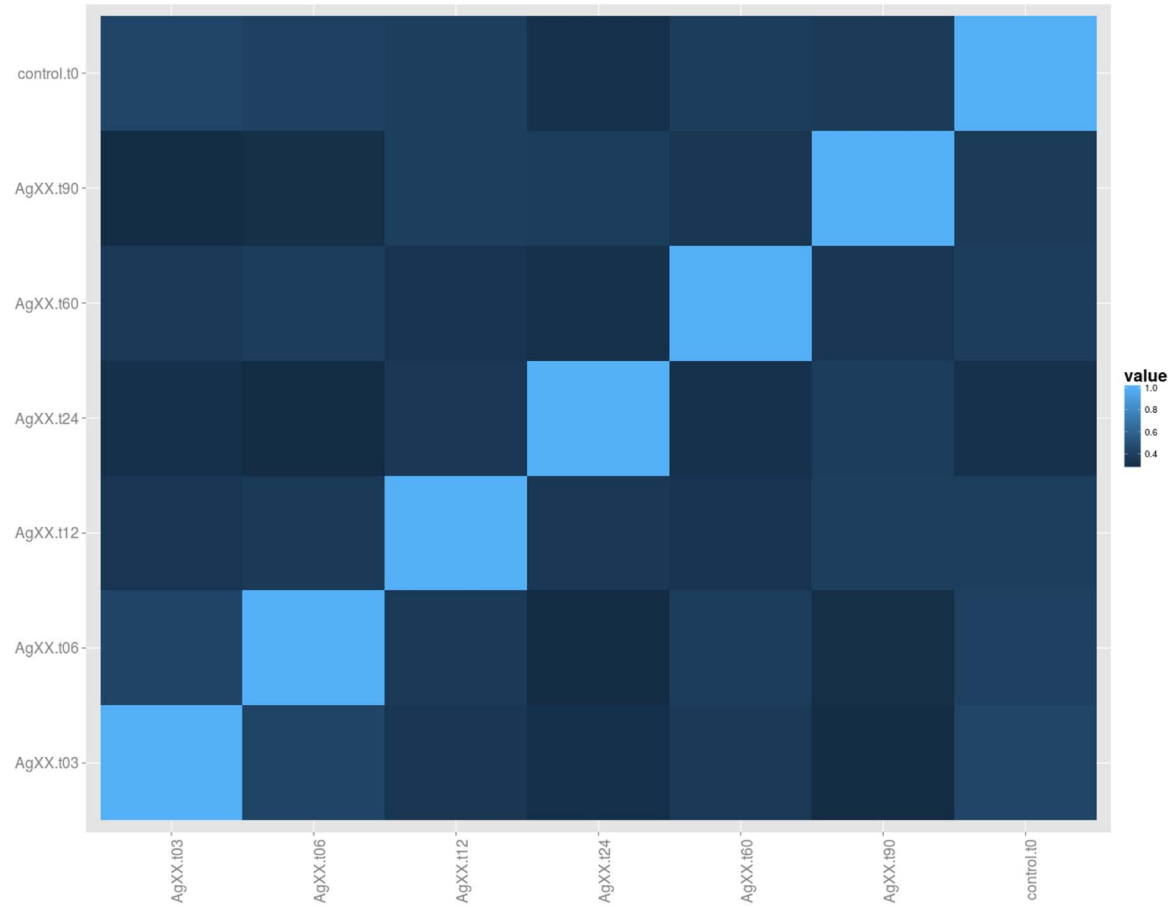

Fig. 2. Correlation matrix of AGXX® metal stress experiments.
Names consist of the metal mesh type and the exposure time in min. Control samples (control.t0) were grown without any metal mesh. Correlation coefficients of the metal stress experiments are color-coded: light blue, perfect positive correlation (+1.0); black, perfect negative (i.e. anti-) correlation (−1.0). (For interpretation of the references to colour in this figure legend, the reader is referred to the web version of this article.)

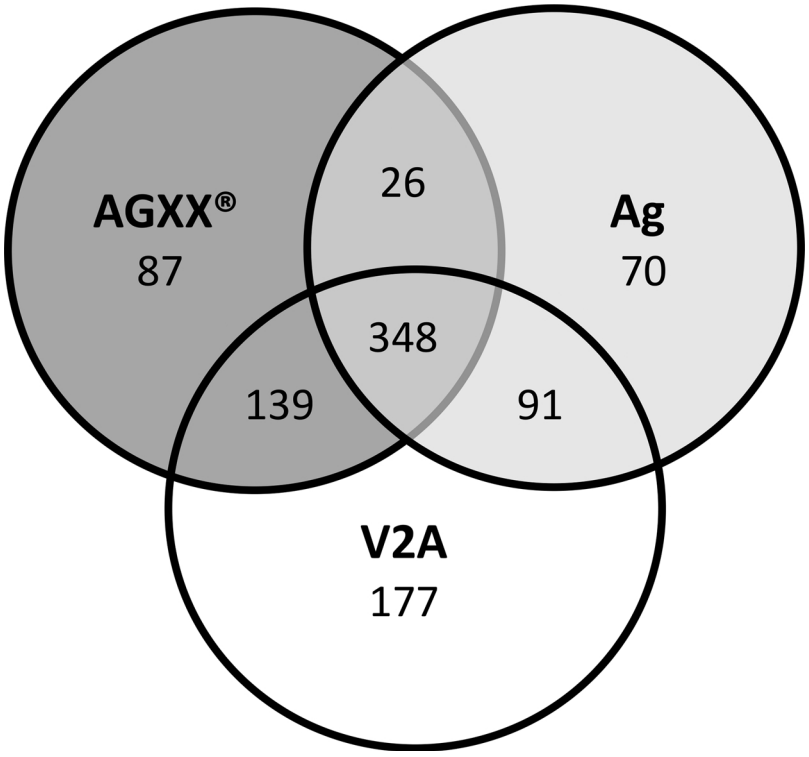

Fig. 3. Venn diagram of differentially expressed genes in *E. faecalis* 12030 exposed for 24 min to V2A, Ag and AGXX®.
The numbers of differentially expressed genes for the three different metal mesh types are shown.

Table 2
Expression of the *cop* operon in *E. faecalis* 12030 exposed to AGXX® versus controls.

Gene number	Gene product (putative)	Expression ratio					
		3 min	6 min	12 min	24 min	60 min	90 min
EF.peg.3041	Transcriptional regulator copper transport operon (CopY)	107.5	165.3	108.0	110.7	22.5	51.2
EF.peg.3040	Copper-translocating P-type ATPase	78.4	147.3	189.6	157.6	36.8	29.9
EF.peg.3039	Copper chaperone/transport protein (CopZ)	8.7	49.6	75.4	106.1	28.3	41.3

peg: Protein encoding gene.

E. coli (Patzer and Hantke, 1998) are part of this group. The second most prevalent COG category was “Transcription” (approx. 11%). The two most prevalent down-regulated COG categories among the 20 down-regulated genes were “Amino acid transport and metabolism” (20%) and “Translation, ribosomal structure and biogenesis” (15%).

3.6. Important role of the cop operon in cellular response to stress induced by AGXX®

The *cop* operon regulates the uptake, availability and export of copper in *E. hirae* and other bacteria (Solioz and Stoyanov, 2003). Its inducibility by Cu^{+}, Cd^{2+} and Ag^{+} has been proven in *E. hirae* (Odermatt et al., 1993). This operon consisting of three genes was strongly induced in *E. faecalis* 12030 exposed to AGXX® (Table 2, see Table A.2 in the Supplementary information for the FDR adjusted *p*-values) and to a lesser extent in cells treated with Ag (Table A.1 in the Supplementary information). This indicates that *cop* plays an important role in the cellular response to metal stress.

The *cop* operon was strongly induced especially at early time-points 3, 6, 12 and 24 min. Upon prolonged exposure (60 and 90 min) the expression ratios declined.

When *E. faecalis* 12030 was exposed to Ag, the *cop* operon was only differentially expressed and up-regulated at time-points 12, 24 and 90 min with a strong induction at the latter time-point (Table A.1 in the Supplementary information). Upon exposure to V2A the *cop* operon genes were not differentially expressed at any time-point (data not shown).

3.7. Induction of heat shock and oxidative stress responses

Special focus was put on genes whose products are important in the cellular response to heat shock, oxidative stress and DNA damage, in order to examine their possible roles in AGXX®-induced metal stress.

Table 3 shows the expression ratios of a selection of heat shock genes coding for chaperones and proteases in *E. faecalis* 12030 exposed to AGXX® versus controls.

Most of the heat shock genes were differentially expressed at time-points 12, 24 and 60 min. Differential expression occurred less frequently and was weaker upon 90 min of exposure to AGXX®. Heat shock genes were mostly up-regulated within a range from approx. 3-fold (*ctsR*, 24 min) to more than 30-fold (*clpB* and *clpE*, 60 min). Only *clpX* and *clpP* were down-regulated but not considered as differentially expressed at any time-point. When the contrast for the calculation of gene expression ratios was changed from AGXX® versus controls to AGXX® versus Ag, differential expression of heat shock genes was very rare. Only *clpE* was differentially expressed at time-points 12 and 60 min with expression ratios of approx. 6 and 9, respectively. All other heat shock genes were not considered as differentially expressed. Overall, the trends of the expression ratios (i.e. up or down- regulation) were similar to those of the contrast AGXX® versus controls, even though their fold changes were smaller (data not shown).

Table 4 shows the expression ratios of a selection of oxidative stress genes coding for oxidoreductases and protective enzymes against ROS in *E. faecalis* 12030 exposed to AGXX® versus controls.

Except for *EF.peg.186* coding for catalase all oxidative stress genes were up-regulated at every time-point and most of them were differentially expressed starting from time-point 6 min *EF.peg.1923* and *EF.peg.1924*- both coding for thioredoxin- were strongly up-regulated at time-points 24 and 60 min.

Similar to the heat shock genes, differential expression of oxidative stress genes was very rare when the contrast was changed from AGXX® versus controls to AGXX® versus Ag. Only *EF.peg.1457* coding for thioredoxin was differentially expressed and up-regulated approx. 31-fold at time-point 60 min. Generally, up regulation was weaker and more down regulation occurred upon prolonged exposure to AGXX®, mostly concerning genes coding for thioredoxin (data not shown).

A selection of SOS response genes, which are typically induced upon DNA damage, was also analyzed for differential expression (Table 5).

The only differentially expressed genes were *EF.peg.2262* coding for LexA, the repressor of the SOS regulon, with an expression ratio of approx. 5 at time-point 24 min and *EF.peg.596* coding for the DNA polymerase IV with an up-regulation of similar magnitude at time-points 24 and 60 min (Table 5).

In the contrast AGXX® versus Ag the SOS response genes listed in Table 5 were not differentially expressed (data not shown).

A graphical illustration of the expression ratios of all 3073 pegs of *E. faecalis* 12030 at time-point 24 min, when gene expression in *E. faecalis* 12030 exposed to AGXX® versus controls differed most from all other time-points (Fig. 2) is depicted in Fig. 4 as a volcano plot.

Among the top up-regulated and differentially expressed genes, heat shock genes and three oxidative stress genes (all of them encoding thioredoxin) dominated. All three genes of the *cop* operon appeared among the highly significant, top up-regulated genes.

3.8. Verification of RNA sequencing data by RT-qPCR

The transcriptional response of *E. faecalis* 12030 exposed to Ag or AGXX® was validated by performing RT-qPCR assays on two genes of the *cop* operon, *copY* and *copZ*, one heat shock gene, *groES*, and one oxidative stress gene, *sodA*, all of which were found to be highly up-regulated upon exposure to AGXX® by RNA sequencing. Twenty-four minutes was selected as the exposure time, as this time-period gave the most significant effect on gene expression in *E. faecalis* 12030 by RNA sequencing. Fig. 5 shows the effect of Ag and AGXX® on the expression of the four genes in *E. faecalis* 12030.

From the RT-qPCR data, differential regulation of the four genes, *copY*, *copZ*, *groES* and *sodA* is evident. All were up-regulated upon 24 min of exposure to AGXX®. Among them, the *cop* operon genes were the most significantly up-regulated. The changes in gene expression as obtained by RT-qPCR are similar to those obtained by RNA sequencing (Tables 2–4).

On exposure to Ag for 24 min, *copY* was ~29-fold up-regulated, a change that proved to be statistically significant (for RNA sequencing data, see Supplementary Table A.1). On the other hand, no significant difference was observed in the expression of the *copZ*, *groES* and *sodA* genes (Fig. 5).

3.9. Detection of AGXX®-mediated generation of hydrogen peroxide

Two metals in electrical contact form a galvanic cell. The AGXX®

Table 3
Expression of heat shock genes in *E. faecalis* 12030 exposed to AGXX® versus controls.

Gene number	Gene product (putative)	Expression ratio					
		3 min	6 min	12 min	24 min	60 min	90 min
Chaperones							
EF.peg.2289	Heat shock protein 60 family chaperone GroEL	1.7	2.9	**8.9**	**16.0**	**7.0**	**4.4**
EF.peg.2290	Heat shock protein 60 family co-chaperone GroES	1.7	3.0	**12.0**	**26.9**	**5.7**	**6.0**
EF.peg.1285	Heat shock protein GrpE	−1.0	2.7	**7.0**	**13.3**	3.1	1.1
EF.peg.1284	Chaperone protein DnaK	1.1	2.6	**6.8**	**14.2**	**5.4**	3.0
EF.peg.1282	Chaperone protein DnaJ	−1.1	1.4	2.8	**7.0**	**5.6**	2.0
Proteases							
EF.peg.272	ATP-dependent Clp protease ATP-binding subunit ClpX*	−1.0	−1.0	−1.4	−2.0	−1.2	−1.2
EF.peg.1416	ATP-dependent Clp protease ATP-binding subunit ClpE	2.5	**5.7**	**21.7**	**21.3**	**32.3**	**5.3**
EF.peg.2807	ATP-dependent Clp protease proteolytic subunit ClpP*	−1.1	−1.7	−5.4	−4.9	−2.2	−1.9
EF.peg.752	ATP-dependent Clp protease ATP-binding protein ClpB*	1.1	1.2	**7.8**	**24.7**	**30.2**	**7.4**
EF.peg.753	ATP-dependent Clp protease ATP-binding protein ClpB*	1.1	1.1	**8.4**	**20.3**	**16.2**	**5.8**
EF.peg.754	ATP-dependent Clp protease ATP-binding protein ClpB*	−1.1	1.8	**10.2**	**18.0**	**16.7**	3.3
	ATP-dependent Clp protease ATP-binding protein ClpB*	1.0	1.4	**8.8**	**21.0**	**21.0**	**5.5**
EF.peg.2796	ATP-dependent Clp protease ATP-binding subunit ClpC	3.0	**5.8**	**9.4**	**4.9**	**3.8**	1.6
EF.peg.2797	Transcriptional regulator CtsR	2.9	**5.0**	**6.2**	**3.2**	**4.5**	1.6

Asterisks mark annotations from the corresponding genes in *E. faecalis* V583. If two or more genes code for the same enzyme, mean expression ratios for each time-point are given in the line where only the gene product is indicated. Statistically significant expression ratios are shown in bold.

surface consists of micro-galvanic elements formed by Ag and Ru. Ag represents the anode and is oxidized to Ag^+-ions or insoluble silver halides (depending on the electrolyte) and Ru represents the cathode. According to the electrochemical series the redox potential of Ag/Ag^+ is more positive than that of Ru/Ru^{3+}. In the presence of chloride ions (Cl^-) the redox potential of Ag shifts to more negative potentials due to the formation of silver chloride (AgCl). In an aqueous environment Ru forms insoluble hydrous oxides (with different oxidation states), which exhibit good catalytic properties with regard to generation and reduction of O_2 (Anastasijević et al., 1992; Metikoš-Huković et al., 2006; Michell et al., 1978) and electrical conductivity (Ryden et al., 1970). The reduction of O_2 can take place in two 2-electrontransfers with H_2O_2 being formed as an intermediate (Wroblowa et al., 1976; Yeager, 1984). Depending on the pH-value two different reactions are possible (Yeager, 1984) that each lead to a pH-shift to the alkaline range. The intermediate steps of the reactions are

$$O_2 + 2H^+ + 2\,e^- > H_2O_2 \quad \text{for acidic solutions} \tag{1}$$

$$O_2 + H_2O + 2\,e^- > OH^- + HO_2^- \quad \text{for alkaline solutions (Yeager, 1984).} \tag{2}$$

The cell voltage of a galvanic cell depends on the material of the electrodes and the composition of the electrolyte. We measured the cell voltage between sheets of Ag and Ru immersed in an electrolyte containing different concentrations of Cl^-. By increasing the concentration of Cl^- from 0 to 1 M the cell voltage increased from 0.132 V to 0.417 V and the formation of AgCl was detected by electrochemical reduction at an Ag electrode. AgCl is reduced to Ag by light or organic molecules such as sugars and alcohols (Møller et al., 2007).

In order to prove the formation of H_2O_2 we built an AGXX®-system consisting of two separated half-cells connected by a salt bridge (Fig. A.1 in the Supplementary information). The half-cells and the salt bridge were filled with xylenol orange dye solution. A red color was observed only in the cathode compartment indicating the formation of H_2O_2 at the Ru cathode. Consistent with reactions (1) and (2) the pH shifted to the alkaline range with a value of 9.2 in the cathode compartment, whereas it remained at the initial value of 5.5 in the anode compartment. From these results we conclude that O_2 is reduced to H_2O_2 at the Ru cathode.

4. Discussion

The tested antimicrobial surface coating is active against a large number of Gram-positive and Gram-negative bacteria including clinical isolates of *Staphylococcus aureus*, *Staphylococcus epidermidis*, *Enterococcus faecium* and *Escherichia coli* (Guridi et al., 2015). *E. faecalis* 12030 was rapidly killed by the coating indicating that the AGXX® mesh-surface to medium-volume ratio of 0.4 caused lethal metal stress. By contrast and as expected, V2A did not show a measurable effect on growth of *E. faecalis* 12030.

The detection of the COG categories “Amino acid transport and metabolism” and “Translation, ribosomal structure and biogenesis” among the down-regulated genes points to inhibition of protein synthesis upon exposure of *E. faecalis* 12030 for 24 min to AGXX®. This

Table 4
Expression of oxidative stress genes in *E. faecalis* 12030 exposed to AGXX® versus controls.

Gene number	Gene product (putative)	Expression ratio					
		3 min	6 min	12 min	24 min	60 min	90 min
EF.peg.1457	Thioredoxin	4.1	**8.4**	3.1	**6.3**	**27.5**	**4.6**
EF.peg.1923	Thioredoxin	1.9	**6.1**	**5.1**	**17.5**	**14.8**	**7.1**
EF.peg.1924	Thioredoxin	1.6	**6.6**	**5.5**	**13.1**	**13.6**	**7.4**
	Thioredoxin	2.5	**7.0**	**4.6**	**12.3**	**18.6**	**6.4**
EF.peg.2136	Superoxide dismutase	4.5	**10.2**	**6.0**	**12.2**	**4.9**	**7.2**
EF.peg.186	Catalase	2.9	3.4	2.5	−1.0	2.1	−2.1
EF.peg.1721	Glutathione biosynthesis bifunctional protein GshF	2.2	3.4	**3.9**	**3.2**	**3.7**	1.8
EF.peg.2785	Glutathione reductase	2.7	3.0	**4.5**	**3.1**	2.1	1.8

If two or more genes code for the same enzyme, mean expression ratios for each time-point are given in the line where only the gene product is indicated. Statistically significant expression ratios are shown in bold.

Table 5
Expression of SOS response genes in *E. faecalis* 12030 exposed to AGXX® versus controls.

Gene number	Gene product (putative)	Expression ratio					
		3 min	6 min	12 min	24 min	60 min	90 min
EF.peg.205	SOS-response repressor and protease LexA	−1.6	−2.0	−1.3	−1.5	−1.1	−1.3
EF.peg.2262	LexA repressor	−1.1	−1.4	1.1	**5.1**	2.7	2.6
EF.peg.436	RecA protein	1.1	1.6	1.6	1.2	1.3	−1.3
EF.peg.596	DNA polymerase IV	1.0	1.9	2.6	**5.3**	**5.4**	1.8

Statistically significant expression ratios are shown in bold.

observation fits well with the antimicrobial activity of the surface coating.

The total number of differentially expressed genes in *E. faecalis* 12030 exposed to the coating increased with exposure time, up to 24 min, emphasizing the time-dependency of the gene expression levels. The fact that almost one fifth of all genes was differentially expressed after 24 min of exposure to the coating demonstrates the huge impact of AGXX® on the transcriptome of *E. faecalis* 12030.

Of all six exposure times 24 min exposure to AGXX® not only resulted in the largest total number of differentially expressed genes but also in the strongest anti-correlation (i.e. largest difference in gene expression) with the mean of the controls.

To verify the RNA sequencing data, RT-qPCR experiments were performed on RNA derived from *E. faecalis* 12030 exposed for 24 min to Ag or AGXX®. Gene expression of the two metal transporters, *copY* and *copZ* (Solioz and Stoyanov, 2003), the heat shock gene *groES* (Layton and Foster, 2005) and *sodA* coding for the oxidative stress-induced superoxide dismutase (Peppoloni et al., 2011) was studied. All four genes were up-regulated under metal stress caused by AGXX®, confirming the RNA sequencing data. The fold changes in gene expression were in the same range for both methods. Only the up-regulation of the two metal transporters was statistically significant.

The four genes were also up-regulated after exposure to Ag for 24 min, albeit that differential expression was much more pronounced in the case of AGXX®. In the case of Ag, only up-regulation of the metal transporter gene *copY* was found to be statistically significant (Fig. 5).

In DNA microarray studies in which the vancomycin-resistant *E. faecalis* V583 or *E. faecalis* OG1RF was subjected to metal stress by growth in the presence of a high concentration of Cu^{2+} (0.05 mM $CuSO_4$) (Abrantes et al., 2011; Reyes-Jara et al., 2010) the *cop* operon genes were the most significantly induced genes of the whole genome. In the metal stress experiments with AGXX® presented here, the *E. faecalis* 12030 *cop* operon was strongly induced at every time-point while for Ag this was only the case in the 90 min sample (Table A.1 in the Supplementary information). As has been demonstrated earlier for *E. hirae*, *cop* is not only inducible by Cu^{2+}- but also by Ag^{+}-ions (Odermatt et al., 1993). A V2A stainless steel mesh coated with AGXX® is composed of the elements Fe, Cr, Ni, C, Ag and Ru, but does not contain Cu. Thus, strong expression of the *cop* operon in *E. faecalis* 12030 treated with the antimicrobial coating is indirect evidence for the generation and release of bioactive Ag^{+}-ions by AGXX®. These Ag^{+}-ions could be initial mediators of the antimicrobial action of the coating. However, the strong antimicrobial activity of AGXX® is not (solely) dependent on the release of free Ag^{+}-ions as we have pointed out previously (Guridi et al., 2015).

EF.peg.596 belongs to the COG category "Replication,

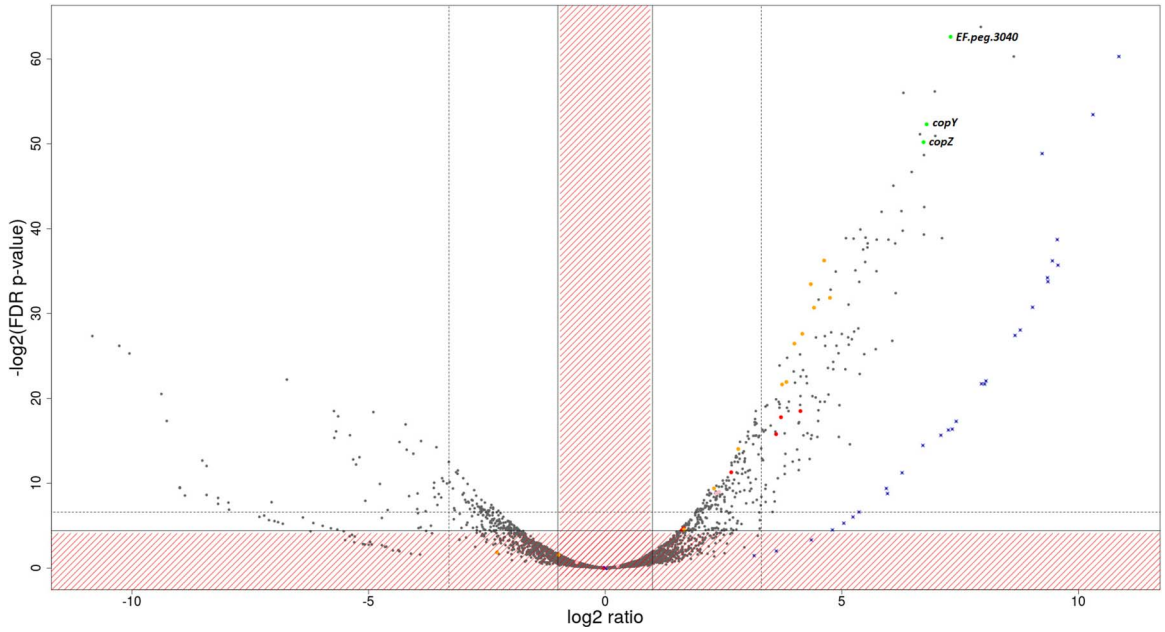

Fig. 4. Volcano plot of the contrast AGXX.t24 versus controls.t0.
The negative log2-transformed false discovery rate (FDR) adjusted *p*-values of all 3073 pegs of *E. faecalis* 12030 are plotted against the log2-transformed expression ratios at time-point 24 min. Statistically significant strongly down- or up-regulated genes are plotted in the upper left or right square denoted by the dashed lines, respectively (FDR adjusted *p*-value < 0.01). Red shaded areas mark FDR adjusted *p*-values > 0.05. Genes whose zero expression values were automatically scaled to noise level to prevent errors as a consequence of having to divide by zero are flagged by a blue cross-sign. The three genes of the *cop* operon are highlighted in green. Genes whose products are important in the response to heat shock are shown in orange. Oxidative stress genes are shown in red and genes induced upon DNA damage as SOS response are colored pink. (For interpretation of the references to colour in this figure legend, the reader is referred to the web version of this article.)

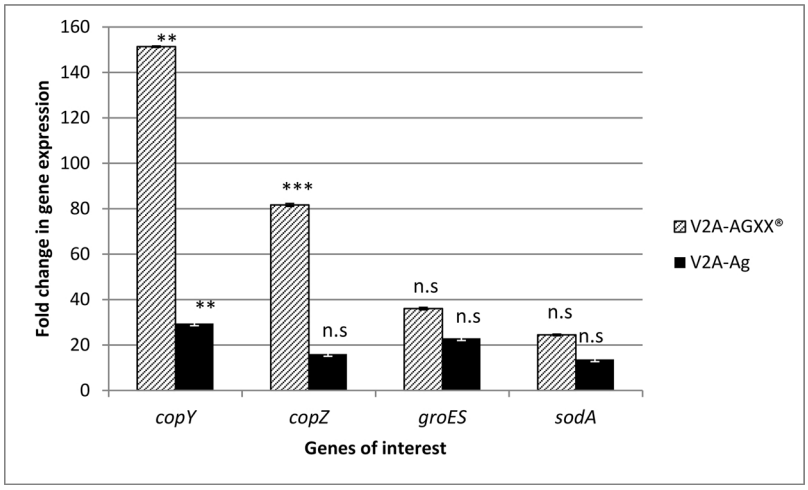

Fig. 5. Differential expression of *copY*, *copZ*, *groES* and *sodA* genes in *E. faecalis* 12030 upon exposure to AGXX® or Ag for 24 min.
Data were normalized to the reference gene *gap* and are shown relative to the control, a culture that was not treated with antimicrobial material. Fold change in gene expression was calculated using the mean value of four RT-qPCR experiments. Error bars indicate the standard deviation. Asterisks indicate the statistical significance, obtained from the *t*-test by SigmaPlot 11.0 (Systat Software, San Jose, CA) (*** $p < 0.001$, ** $p < 0.01$ and n.s means non-significant).

recombination and repair"; it codes for DNA polymerase IV. This enzyme is part of the late cellular SOS response in *E. coli* and the corresponding gene is induced upon DNA damage or collapse of replication forks (Michel, 2005; van der Veen and Abee, 2011). *EF.peg.596* was up-regulated more than 5-fold upon prolonged (24 and 60 min) exposure of *E. faecalis* 12030 to AGXX®. This might well mark the end of an SOS response because *EF.peg.2262*, encoding the LexA repressor of the SOS regulon, was up-regulated starting from 24 min onward. Hence, DNA damage might also play a role in the antimicrobial action of the coating.

Upon exposure of *E. faecalis* 12030 to AGXX® for 12, 24 and 60 min, elevated expression levels of heat shock genes coding for chaperones and Clp proteases were detected. Afterwards, their expression decreased (Table 3). Interestingly, also *EF.peg.2797* was up-regulated. This gene encodes the transcriptional repressor CtsR, a regulator of stress and heat shock response that controls *clp* and molecular chaperone gene expression in Gram-positive bacteria (Derré et al., 1999). A CtsR binding site is present upstream of *clp* and other heat shock genes of several Gram-positive bacteria, such as *E. faecalis*, an indication that CtsR-mediated heat shock regulation is highly conserved in these organisms (Derré et al., 1999). In *E. faecalis* 12030 exposed to the coating, only the ClpP-encoding *EF.peg.2807* was statistically significantly down-regulated. All other heat shock genes, e.g. *EF.peg.2796* (*clpC*) and *EF.peg.1416* (*clpE*) were up-regulated. In fact, *EF.peg.1416* was one of the most strongly induced heat shock genes (Table 3). This indicates that the regulation of expression of *clp* and other heat shock genes in *E. faecalis* 12030 is not (only) dependent on CtsR or that it acts as an activator instead of a repressor in this *E. faecalis* strain.

Not all analyzed heat shock genes were up-regulated in *E. faecalis* 12030 exposed to AGXX®. Expression of *EF.peg.272* and *EF.peg.2807* was reduced (but not considered as differentially expressed due to FDR adjusted *p*-values > 0.05, data not shown) up to approx. 5-fold at time-point 24 min (Table 3). These two genes code for the ClpX ATPase and ClpP peptidase subunit, respectively, of the bacterial ClpXP protease complex. A proteomic study in *E. coli* suggested that reduced degradation by ClpXP, which controls the levels of many stress response proteins, contributes to survival (Neher et al., 2006).

Moreover, it has been shown that the level of DNA polymerase IV, which is involved in the bacterial SOS response, is positively affected by the heat shock chaperone GroE in *E. coli* (Layton and Foster, 2005). The two subunits of *E. coli* GroE are encoded by the genes *groEL* and *groES* (Layton and Foster, 2005). The corresponding genes were strongly up-regulated in *E. faecalis* 12030 exposed to the coating. In agreement with the interrelationships between the heat shock and SOS responses, the down-regulation of *clpX* and *clpP* and the up- regulation of *groEL, groES* and *EF.peg.596* (DNA polymerase IV) in AGXX®-exposed *E. faecalis* 12030 could decrease degradation of certain stress proteins, e.g. heat shock and oxidative stress proteins – and SOS response proteins such as DNA polymerase IV – in the struggle to withstand the antimicrobial action of the coating.

Exposure to AGXX® elicits a (much) stronger stress response in *E. faecalis* 12030 than exposure to Ag, which suggests that AGXX® is superior to conventional Ag coatings in terms of impact on the transcriptome and triggering a broad stress response but, ultimately, antimicrobial activity.

Almost all oxidative stress genes were up-regulated upon exposure of *E. faecalis* 12030 to the coating. The highest fold changes were seen for the thioredoxin genes. Notably, *EF.peg.1457* was the only differentially expressed and strongly up-regulated (30-fold at time-point 60 min) oxidative stress gene in the contrast AGXX® versus Ag (data not shown). Thioredoxin is the major ubiquitous disulfide reductase responsible for keeping proteins in their reduced state (Arnér and Holmgren, 2000). The observed up-regulation of oxidative stress genes strongly suggests that oxidation of cellular components, especially proteins, takes place either by AGXX® itself or by antimicrobial intermediates such as ROS that are generated by the coating. Oxidation of proteins could lead to protein denaturation and ultimately to the induction of the observed heat shock-like cellular response.

The gene *EF.peg.2136* putatively encoding superoxide dismutase (99% amino acid sequence identity with the characterized gene product in *E. faecalis* JH2-2 (Bizzini et al., 2009)) was clearly up-regulated and differentially expressed in AGXX®-exposed *E. faecalis* 12030. Superoxide dismutase catalyzes the detoxification of highly reactive superoxide anions (O_2^-) into the less reactive hydrogen peroxide (H_2O_2) and molecular oxygen. Both O_2^- and H_2O_2 likely contribute to the antimicrobial activity of the coating, e.g. by oxidation of proteins, nucleic acids and phospholipids. In accordance, also the catalase gene *EF.peg.186*, involved in the decomposition of H_2O_2 (demonstrated for *E. faecalis* V583 KatA (Frankenberg et al., 2002), amino acid sequence identity with *E. faecalis* 12030 KatA 99% (Frankenberg et al., 2002)), was up-regulated at most of the time-points after AGXX® addition.

Further ROS, e.g. hydroxyl radicals (OH·), could be generated by AGXX® in a Fenton-type reaction with silver in a similar way as proposed for copper (Solioz and Stoyanov, 2003)

$$Ag^+ + 2\ GSH = 2\ Ag + GSSG + 2H^+ \quad (3)$$

$$Ag + H_2O_2 = Ag^+ + OH^- + OH\cdot \text{ (Ono et al., 1977)} \quad (4)$$

The combined reactions (3) and (4) could cause redox cycling of silver at the expense of glutathione (GSH) to produce reduced GSSG, as described for copper (Klotz and Weser, 1998). In fact, *EF.peg.1721* encoding the putative glutathione biosynthesis bifunctional protein GshF (or glutathione synthetase) (99% amino acid sequence identity with the characterized glutathione synthetase from *E. faecalis* V583 (Janowiak

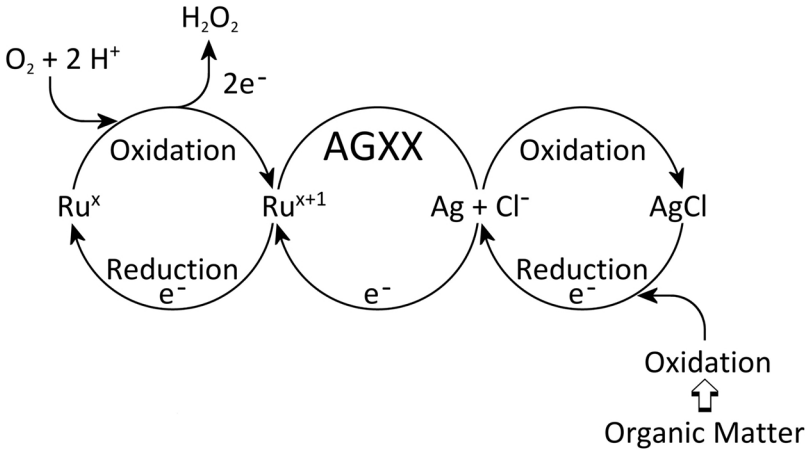

Fig. 6. Redox-cycling and self-renewal of AGXX®.
The postulated mechanism of action of the coating is based on two interconnected redox-cycles resulting in the long-term antimicrobial effect including self-renewal of the material. Elementary Ag is oxidized to Ag^+ by Cl^- present in the electrolyte. Subsequently, oxidation of organic matter, such as sugars in the bacteria, leads to reduction of AgCl. At the same time higher valent Ru^{x+1} is reduced to lower valent Ru^x. Reduction of O_2 results in the formation of H_2O and H_2O_2, and at the same time lower valent Ru^x is oxidized to its initial state by O_2.

et al., 2006)) and *EF.peg.2785*, coding for glutathione reductase (100% amino acid sequence identity with glutathione reductase from *E. faecalis* V583 (Patel et al., 1998)), were up-regulated approx. 2- to 4-fold, providing evidence for the consumption of GSH.

We postulate that ruthenium – the other metal component of the coating – is also involved in the redox (cycling) reactions (Fig. 6). These reactions could take place in *E. faecalis* 12030 exposed to AGXX® because (indirect) evidence was obtained for the generation and release of Ag^+-ions by AGXX®. Cu^+ bound to the copper chaperone/transport protein CopZ is solvent exposed (Cobine et al., 1999) and, thus, this copper ion could participate in Fenton-type reactions (Solioz and Stoyanov, 2003). As the *cop* operon is also inducible by Ag^+ (Odermatt et al., 1993), binding and exposure of Ag^+ in a similar way could lead to analogous chemical reactions.

We suggest a mechanism relying on two interconnected redox-cycles to explain the long-term antimicrobial effect including self-renewal of the antimicrobial coating (Fig. 6). Elementary Ag is oxidized by Cl^- present in the electrolyte. Subsequently, oxidation of organic matter such as sugars leads to reduction of AgCl. At the same time higher valent Ru^{x+1} is reduced to lower valent Ru^x. The reduction of O_2 results in the formation of H_2O and H_2O_2, and at the same time lower valent Ru^x will be oxidized to its initial state by O_2. We assume that chemical reactions of H_2O_2 at the AGXX® surface generate further ROS such as superoxide radicals.

Notably, a correlation was seen between induction of the *cop* operon and expression of oxidative stress as well as heat shock genes in *E. faecalis* 12030 exposed to the coating. The *cop* operon was strongly induced at time-points 3, 6, 12 and 24 min while oxidative stress genes were up-regulated at time-points 6, 12, 24 and 60 min and heat shock genes at time-points 12, 24 and 60 min. The slight delay seen for the oxidative and heat shock stress responses might be explained by the time required for the occurrence of redox reactions and the interactions between silver ions and cellular components, respectively, and the subsequent induction of signaling and regulation pathways.

The main events – release of free Ag^+-ions and generation of ROS by AGXX®, oxidation of cellular components as well as co-induction of heat shock and oxidative stress response – could be interlinked as a series of parallel or successive events leading to the strong antimicrobial effect of the coating.

In terms of response to metal stress, the best-studied bacterium is *E. coli* (Zhang et al., 2016). Under elevated Cu^+ and Ag^+ concentrations, the *E. coli* two-component system CusR/CusS induces expression of genes involved in metal efflux (Gudipaty et al., 2012). The *cusS* gene is important for developing resistance to Cu^+ and Ag^+ and is required for Cu^+ and Ag^+ dependent up-regulation of *cusCFBA* expression (Gudipaty et al., 2012). Copper and silver ions induce expression of *copA* (Rensing et al., 2000), the central component of the copper homeostasis system in *E. coli*, CopA removes excess Cu^+ from the cytoplasm. Intracellular Cu^+ and Ag^+ levels activate CueR, which regulates *copA* (Rensing and Grass, 2003).

McQuillan et al. studied the adaptive stress response of *E. coli* to exposure to silver in two different forms, (i) Ag^+ in solution and (ii) Ag^+ delivered locally to the outer membrane as Ag nanoparticles. They examined the stress response by monitoring transcription levels of *copA*, *cueO*, *cusA* and *cusR* by RT-qPCR. Differential gene expression on exposure to Ag^+ and Ag nanoparticles with a more pronounced up-regulation of *copA*, *cueO* and *cusA*, encoding Cu homeostasis and resistance proteins, for Ag nanoparticles was observed (McQuillan et al., 2012). A microarray-based study, applying silver as silver nitrate or as Ag-nanoparticles, revealed that in total 188 *E. coli* genes were differentially expressed by both treatments. Out of these 188 genes, 161 were up-regulated while 27 genes were down-regulated. The expression of 19 heat shock response genes, including *clpB*, *dnaK, dnaJ, grpE, groES, groEL,* and *lon* was highly induced by silver. In addition, silver ions induced a redox stress response linked with a 4600-fold up-regulation of *soxS* (McQuillan and Shaw, 2014), a transcription factor activating the expression of the superoxide dismutase gene *sodA* (Baez and Shiloach, 2013). Copper homeostasis-related genes were also up-regulated, indicating that Ag^+ ions can also activate copper signaling (McQuillan and Shaw, 2014).

Our study demonstrated that the transcriptome of *E. faecalis* 12030 is highly affected by the antimicrobial coating. After 24 min exposure to AGXX®, 19.5% of the *E. faecalis* 12030 genome showed differential gene expression. Of total 600 differentially expressed genes, 373 genes were observed to be up-regulated and 227 genes were down-regulated.

In summary, both in *E. coli* and *E. faecalis*, copper homeostasis genes, heat shock and oxidative stress genes were differentially expressed under silver stress. Interestingly, expression level changes were found to vary considerably between the different application forms of the metal.

5. Conclusions

The novel antimicrobial surface coating rapidly kills growing *E. faecalis*. RNA sequencing and RT-qPCR revealed that AGXX® had a large impact on the transcriptome of *E. faecalis* 12030. Strong induction of the *cop* operon provided indirect evidence for the presence of free Ag^+-ions released by the coating. They are likely initial mediators of the antimicrobial action of the coating as a correlation exists between the presence of Ag^+-ions and induction of oxidative stress as well as heat shock responses. Strong up-regulation of chaperone and protease genes suggests that a heat shock-like situation exists. Additionally, the up-regulation of genes encoding oxidoreductases and ROS-protective enzymes points to a high level of oxidative stress due to ROS such as H_2O_2. ROS generation could be catalytically supported by redox reactions at the ruthenium micro cathodes on the AGXX® surface. ROS might be the

major antimicrobial agents, causing oxidative damage to vital cellular components such as proteins, nucleic acids and lipids. Taken together, we propose that the release of Ag^+-ions and the generation of H_2O_2 and other ROS lead to a synergistic, antimicrobial effect of AGXX® that is superior to that of conventional Ag coatings.

Acknowledgments

This research was funded by German Aerospace Center (DLR) grants 50WB1166 and 50WB1466. The funders had no involvement in study design, the collection, analysis and interpretation of data, the writing of the report and the decision to submit the article for publication.

Appendix A. Supplementary data

Supplementary data associated with this article can be found, in the online version, at http://dx.doi.org/10.1016/j.micres.2017.11.006.

References

Aakra, A., VebØ, H., Snipen, L., Hirt, H., Aastveit, A., Kapur, V., Dunny, G., Murray, B., Nes, I.F., 2005. Transcriptional response of *Enterococcus faecalis* V 583 to erythromycin. Antimicrob. Agents Chemother. 49 (6), 2246–2259.

Aakra, A., VebØ, H., Indahl, U., Snipen, L., Gjerstad, Ø., Lunde, M., Nes, I.F., 2010. The response of *Enterococcus faecalis* V 583 to chloramphenicol treatment. Int. J. Microbiol. 2010, 483048. http://dx.doi.org/10.1155/2010/483048.

Abrantes, M.C., Lopes, M., de, F., Kok, J., 2011. Impact of manganese, copper and zinc ions on the transcriptome of the nosocomial pathogen *Enterococcus faecalis* V583. PLoS One 6, e26519. http://dx.doi.org/10.1371/journal.pone.0026519.

Abrantes, M.C., Kok, J., de F. Lopesa, M., 2013. EfaR is a major regulator of *Enterococcus faecalis* manganese transporters and influences processes involved in host colonization and infection. Infect. Immun. 81, 935–944. http://dx.doi.org/10.1128/IAI.06377-11.

Agranoff, D.D., Krishna, S., 1998. Metal ion homeostasis and intracellular parasitism. Mol. Microbiol. 28 (3), 403–412. http://dx.doi.org/10.1046/j.1365-2958.1998.00790.x.

Alexander, J.W., 2009. History of the medical use of silver. Surg. Infect. 10, 289–292. http://dx.doi.org/10.1089/sur.2008.9941.

Anastasijević, N., Dimitrijević, Z.M., Adžić, R.R., 1992. Oxygen reduction on a modified ruthenium electrode. Electrochim. Acta 37, 457–464. http://dx.doi.org/10.1016/0013-4686(92)87036-Y.

Arnér, E.S.J., Holmgren, A., 2000. Physiological functions of thioredoxin and thioredoxin reductase. Eur. J. Biochem. 267 (20), 6102–6109. http://dx.doi.org/10.1046/j.1432-1327.2000.01701.x.

Aziz, R.K., Bartels, D., Best, A.a., DeJongh, M., Disz, T., Edwards, R.a., Formsma, K., Gerdes, S., Glass, E.M., Kubal, M., Meyer, F., Olsen, G.J., Olson, R., Osterman, A.L., Overbeek, R.a., McNeil, L.K., Paarmann, D., Paczian, T., Parrello, B., Pusch, G.D., Reich, C., Stevens, R., Vassieva, O., Vonstein, V., Wilke, A., Zagnitko, O., 2008. The RAST Server: rapid annotations using subsystems technology. BMC Genom. 9, 75. http://dx.doi.org/10.1186/1471-2164-9-75.

Baez, A., Shiloach, A., 2013. *Escherichia coli* avoids high dissolved oxygen stress by activation of SoxRS and manganese superoxide dismutase. Microb. Cell Factories 12 (23). http://dx.doi.org/10.1186/1475-2859-12-23.

Bizzini, A., Zhao, C., Auffray, Y., Hartke, A., 2009. The *Enterococcus faecalis* superoxide dismutase is essential for its tolerance to vancomycin and penicillin. J. Antimicrob. Chemother. 64. http://dx.doi.org/10.1093/jac/dkp369.

Bouchard, A., 2011. AgXX glass microspheres, In vitro evaluation of cytotoxicity by neutral red assay using MRC-5 cell line with a direct contact procedure. Report 20100326STP. CERB, Baugy, France (Sponsor: APOGEPHA Arzneimittel GmbH Dresden, Germany).

Butala, M., Žgur-Bertok, D., Busby, S.J.W., 2009. The bacterial LexA transcriptional repressor. Cell. Mol. Life Sci. 66 (1), 82–93. http://dx.doi.org/10.1007/s00018-008-8378-6.

Cobine, P., Wickramasinghe, W.A., Harrison, M.D., Weber, T., Solioz, M., Dameron, C.T., 1999. The *Enterococcus hirae* copper chaperone CopZ delivers copper(I) to the CopY repressor. FEBS Lett. 445, 27–30. http://dx.doi.org/10.1016/S0014-5793(99)00091-5.

Costerton, J.W., Stewart, P.S., Greenberg, E.P., 1999. Bacterial biofilms: a common cause of persistent infections. Science 80- (284), 1318–1322. http://dx.doi.org/10.1126/science.284.5418.1318.

Cox, M.M., 2007. Regulation of bacterial RecA protein function. Crit. Rev. Biochem. Mol. Biol. 42, 41–63. http://dx.doi.org/10.1080/10409230701260258.

de Jong, A., van der Meulen, S., Kuipers, O.P., Kok, J., 2015. T-REx: transcriptome analysis webserver for RNA-seq expression data. BMC Genom. 16, 663. http://dx.doi.org/10.1186/s12864-015-1834-4.

Derré, I., Rapoport, G., Msadek, T., 1999. CtsR, a novel regulator of stress and heat shock response, controls *clp* and molecular chaperone gene expression in Gram-positive bacteria. Mol. Microbiol. 31, 117–131. http://dx.doi.org/10.1046/j.1365-2958.1999.01152.x.

Edgar, R., Domrachev, M., Lash, A.E., 2002. Gene Expression Omnibus: NCBI gene expression and hybridization array data repository. Nucleic Acids Res. 30, 207–210. http://dx.doi.org/10.1093/nar/30.1.207.

Franke, S., Grass, G., Rensing, C., Nies, D.H., 2003. Molecular analysis of the copper-transporting efflux system CusCFBA of *Escherichia coli*. J. Bacteriol. 185, 3804–3812. http://dx.doi.org/10.1128/JB.185.13.3804-3812.2003.

Frankenberg, L., Brugna, M., Hederstedt, L., 2002. *Enterococcus faecalis* heme-dependent catalase. J. Bacteriol. 184, 6351–6356. http://dx.doi.org/10.1128/JB.184.22. (6351-6356.2002).

Gilmore, M.S., Clewell, D.B., Ike, Y., Shankar, N., 2014. Enterococci From Commensals to Leading Causes of Drug Resistant Infection.

Gordon, O., Slenters, T.V., Brunetto, P.S., Villaruz, A.E., Sturdevant, D.E., Otto, M., Landmann, R., Fromm, K.M., 2010. Silver coordination polymers for prevention of implant infection: thiol interaction, impact on respiratory chain enzymes, and hydroxyl radical induction. Antimicrob. Agents Chemother. 54, 4208–4218. http://dx.doi.org/10.1128/AAC.01830-09.

Grass, G., Rensing, C., Solioz, M., 2011. Metallic copper as an antimicrobial surface. Appl. Environ. Microbiol. 77 (5), 1541–1547. http://dx.doi.org/10.1128/AEM.02766-10.

Gudipaty, S.A., Larsen, A.S., Rensing, C., McEvoy, M.M., 2012. Regulation of Cu(I)/Ag(I) efflux genes in *Escherichia coli* by the sensor kinase CusS. FEMS Microbiol. Lett. 330 (1), 30–37. http://dx.doi.org/10.1111/j.1574-6968.2012.02529.x.

Gupta, B.L., 1973. Microdetermination techniques for H_2O_2 in irradiated solutions. Microchem. J. 18, 363–374. http://dx.doi.org/10.1016/0026-265X(73)90059-3.

Guridi, A., Diederich, A.-K., Aguila-Arcos, S., Garcia-Moreno, M., Blasi, R., Broszat, M., Schmieder, W., Clauss-Lendzian, E., Sakinc-Gueler, T., Andrade, R., Alkorta, I., Meyer, C., Landau, U., Grohmann, E., 2015. New antimicrobial contact catalyst killing antibiotic resistant clinical and waterborne pathogens. Mater. Sci. Eng. C 50, 1–11. http://dx.doi.org/10.1016/j.msec.2015.01.080.

Hartl, F.U., Bracher, A., Hayer-Hartl, M., 2011. Molecular chaperones in protein folding and proteostasis. Nature 475, 324–332. http://dx.doi.org/10.1038/nature10317.

Hidron, A.I., Edwards, J.R., Patel, J., Horan, T.C., Sievert, D.M., Pollock, D.A., Fridkin, S.K., Natl Healthcare Safety Network, T., Participating Natl Healthcare, S., 2008. Antimicrobial-resistant pathogens associated with healthcare-associated infections: annual summary of data reported to the National Healthcare Safety Network at the Centers for Disease Control and Prevention, 2006–2007. Infect. Control Hosp. Epidemiol. 29, 996–1011. http://dx.doi.org/10.1086/591861.

Huebner, J., Wang, Y., Krueger, W.A., Madoff, L.C., Martirosian, G., Boisot, S., Goldmann, D.A., Kasper, D.L., Tzianabos, A.O., Pier, G.B., 1999. Isolation and chemical characterization of a capsular polysaccharide antigen shared by clinical isolates of *Enterococcus faecalis* and vancomycin-resistant *Enterococcus faecium*. Infect. Immun. 67, 1213–1219.

Imlay, J. a, 2003. Pathways of oxidative damage. Annu. Rev. Microbiol. 57, 395–418. http://dx.doi.org/10.1146/annurev.micro.57.030502.090938.

Kittleson, J.T., Loftin, I.R., Hausrath, A.C., Engelhardt, K.P., Rensing, C., McEvoy, M.M., 2006. Periplasmic metal-resistance protein CusF exhibits high affinity and specificity for both CuI and AgI. Biochemistry 45, 11096–11102. http://dx.doi.org/10.1021/bi0612622.

Klotz, L.-O., Weser, U., 1998. In: Rainsford, K.D., Milanino, R., Sorenson, J.R.J., Velo, G.P. (Eds.), Biological Chemistry of Copper Compounds BT – Copper and Zinc in Inflammatory and Degenerative Diseases. Springer, Netherlands, Dordrecht, pp. 19–46. http://dx.doi.org/10.1007/978-94-011-3963-2_3.

Landau, U., 2013. AGXX – Eine nachhaltige Lösung für die Entkeimung wässriger Lösungen. Galvanotechnik 11, 2169–2184.

Langmead, B., Salzberg, S.L., 2012. Fast gapped-read alignment with bowtie 2. Nat. Methods 9, 357–359. http://dx.doi.org/10.1038/nmeth.1923.

Lansdown, A.B.G., 2006. Silver in health care: antimicrobial effects and safety in use. Curr. Probl. Dermatol. 33, 17–34. http://dx.doi.org/10.1159/000093928.

Lansdown, A.B.G., 2010. A pharmacological and toxicological profile of silver as an antimicrobial agent in medical devices. Adv. Pharmacol. Sci. http://dx.doi.org/10.1155/2010/910686.

Layton, J.C., Foster, P.L., 2003. Error-prone DNA polymerase IV is controlled by the stress-response sigma factor, RpoS, in *Escherichia coli*. Mol. Microbiol. 50, 549–561. http://dx.doi.org/10.1046/j.1365-2958.2003.03704.x.

Layton, J.C., Foster, P.L., 2005. Error-prone DNA polymerase IV is regulated by the heat shock chaperone GroE in *Escherichia coli*. J. Bacteriol. 187, 449–457. http://dx.doi.org/10.1128/JB.187.2.449-457.2005.

Lewis, K., 2001. Riddle of biofilm resistance. Antimicrob. Agents Chemother. http://dx.doi.org/10.1128/AAC.45.4.999-1007.2001.

Li, H., Handsaker, B., Wysoker, A., Fennell, T., Ruan, J., Homer, N., Marth, G., Abecasis, G., Durbin, R., 2009. The sequence alignment/map format and SAMtools. Bioinformatics 25, 2078–2079. http://dx.doi.org/10.1093/bioinformatics/btp352.

Livak, K.J., Schmittgen, T.D., 2001. Analysis of relative gene expression data using real time quantitative PCR and the 2DDCT method. Methods 25 (4), 402–408. http://dx.doi.org/10.1006/meth.2001.1262.

Loftin, I.R., Franke, S., Blackburn, N.J., McEvoy, M.M., 2007. Unusual Cu(I)/Ag(I) coordination of *Escherichia coli* CusF as revealed by atomic resolution crystallography and X-ray absorption spectroscopy. Protein Sci. 16, 2287–2293. http://dx.doi.org/10.1110/ps.073021307.

Lusetti, S.L., Cox, M.M., 2002. The bacterial RecA protein and the recombinational DNA repair of stalled replication forks. Annu. Rev. Biochem. 71, 71–100. http://dx.doi.org/10.1146/annurev.biochem.71.083101.133940.

Møller, P., Hilbert, L.R., Corfitzen, C.B., Albrechtsen, H.-J., 2007. A new approach for biologically-Inhibiting surfaces. J. Appl. Surf. Finish. 149–157.

Maillard, J.-Y., Hartemann, P., 2012. Silver as an antimicrobial: facts and gaps in knowledge. Crit. Rev. Microbiol. 39, 1–11. http://dx.doi.org/10.3109/1040841X.2012.713323.

Mattoo, R.U.H., Goloubinoff, P., 2014. Molecular chaperones are nanomachines that

catalytically unfold misfolded and alternatively folded proteins. Cell. Mol. Life Sci. 71 (17), 3311–3325. http://dx.doi.org/10.1007/s00018-014-1627-y.
McQuillan, J.S., Shaw, A.M., 2014. Differential gene regulation in the Ag nanoparticle and Ag(+)-induced silver stress response in *Escherichia coli*: a full transcriptomic profile. Nanotoxicology 5390, 1–8. http://dx.doi.org/10.3109/17435390.2013.870243.
McQuillan, J.S., Infante, H.G., Stokes, E., Shaw, A.M., 2012. Silver nanoparticle enhanced silver ion stress response in *Escherichia coli* K12. Nanotoxicology 6, 857–866. http://dx.doi.org/10.3109/17435390.2011.626532.
Metikoš-Huković, M., Babić, R., Jović, F., Grubač, Z., 2006. Anodically formed oxide films and oxygen reduction on electrodeposited ruthenium in acid solution. Electrochim. Acta 51, 1157–1164. http://dx.doi.org/10.1016/j.electacta.2005.05.029.
Michel, B., 2005. After 30 years of study, the bacterial SOS response still surprises us. PLoS Biol. 3 (7). http://dx.doi.org/10.1371/journal.pbio.0030255.
Michell, D., Rand, D.A.J., Woods, R., 1978. A study of ruthenium electrodes by cyclic voltammetry and X-ray emission spectroscopy. J. Electroanal. Chem. Interfacial Electrochem. 89, 11–27. http://dx.doi.org/10.1016/S0022-0728(78)80027-8.
Mijnendonckx, K., Leys, N., Mahillon, J., Silver, S., Van Houdt, R., 2013. Antimicrobial silver: uses, toxicity and potential for resistance. BioMetals 26, 609–621. http://dx.doi.org/10.1007/s10534-013-9645-z.
Mohamed, J.A., Huang, D.B., 2007. Biofilm formation by enterococci. J. Med. Microbiol. 56 (Pt 12), 1581–1588. http://dx.doi.org/10.1099/jmm.0.47331-0.
Neher, S.B., Villén, J., Oakes, E.C., Bakalarski, C.E., Sauer, R.T., Gygi, S.P., Baker, T.A., 2006. Proteomic profiling of ClpXP substrates after DNA damage reveals extensive instability within SOS regulon. Mol. Cell 22, 193–204. http://dx.doi.org/10.1016/j.molcel.2006.03.007.
Odermatt, A., Solioz, M., 1995. Two trans-acting metalloregulatory proteins controlling expression of the copper-ATPases of *Enterococcus hirae*. J. Biol. Chem. 270, 4349–4354. http://dx.doi.org/10.1074/jbc.270.9.4349.
Odermatt, A., Suter, H., Krapf, R., Solioz, M., 1993. Primary structure of two P-type ATPases involved in copper homeostasis in *Enterococcus hirae*. J. Biol. Chem. 268, 12775–12779.
Odermatt, A., Krapf, R., Solioz, M., 1994. Induction of the putative copper ATPases, CopA and CopB, of *Enterococcus hirae* by Ag^{+} and Cu^{2+}, and Ag^{+} extrusion by CopB. Biochem. Biophys. Res. Commun. 202, 44–48. http://dx.doi.org/10.1006/bbrc.1994.1891.
Ono, Y., Matsumura, T., Kitajima, N., Fukuzumi, S., 1977. Formation of superoxide ion during the decomposition of hydrogen peroxide on supported metals. J. Phys. Chem. 81, 1307–1311. http://dx.doi.org/10.1021/j100528a018.
Park, H., Kim, J.J.Y., Kim, J.J.Y., Lee, J., Hahn, J.-S., Gu, M.B., Yoon, J., Yeon, J., Kim, J.J.Y., Lee, J., Hahn, J.-S., Bock, M., Yoon, J., 2009. Silver-ion-mediated reactive oxygen species generation affecting bactericidal activity. Water Res. 43, 1027–1032. http://dx.doi.org/10.1016/j.watres.2008.12.002.
Patzer, S.I., Hantke, K., 1998. The ZnuABC high-affinity zinc uptake system and its regulator Zur in *Escherichia coli*. Mol. Microbiol. 28, 1199–1210. http://dx.doi.org/10.1046/j.1365-2958.1998.00883.x.
Peppoloni, S., Posteraro, B., Colombari, B., Manca, L., Hartke, A., Giard, J.C., Sanguinetti, M., Fadda, G., Blasi, E., 2011. Role of the (Mn)superoxide dismutase of *Enterococcus faecalis* in the in vitro interaction with microglia. Microbiology 157, 1816–1822.
Prabhu, S., Poulose, E.K., 2012. Silver nanoparticles: mechanism of antimicrobial action, synthesis, medical applications, and toxicity effects. Int. Nano Lett. 2, 32. http://dx.doi.org/10.1186/2228-5326-2-32.
Rensing, C., Fan, B., Sharma, R., Mitra, B., Rosen, B.P., 2000. CopA: An *Escherichia coli* Cu(I)-translocatingP-type ATPase. PNAS 97 (2), 652–656.
Rensing, C., Grass, G., 2003. *Escherichia coli* mechanisms of copper homeostasis in a changing environment. FEMS Microbiol. Rev. 27, 197–213.
Reyes-Jara, A., Latorre, M., Lopez, G., Bourgogne, A., Murray, B.E., Cambiazo, V., Gonzalez, M., 2010. Genome-wide transcriptome analysis of the adaptive response of *Enterococcus faecalis* to copper exposure. Biometals 23, 1105–1112. http://dx.doi.org/10.1007/s10534-010-9356-7.
Robinson, M.D., McCarthy, D.J., Smyth, G.K., 2010. edgeR: a Bioconductor package for differential expression analysis of digital gene expression data. Bioinformatics 26, 139–140. http://dx.doi.org/10.1093/bioinformatics/btp616.
Ryden, W.D., Lawson, A.W., Sartain, C.C., 1970. Electrical transport properties of IrO_2 and RuO_2. Phys. Rev. B 1, 1494–1500. http://dx.doi.org/10.1103/PhysRevB.1.1494.
Sahm, D.F., Olsen, L., 1990. In vitro detection of enterococcal vancomycin resistance. Antimicrob. Agents Chemother. 34, 1846–1848. http://dx.doi.org/10.1128/AAC.34.9.1846.
Solioz, M., Stoyanov, J.V., 2003. Copper homeostasis in *Enterococcus hirae*. FEMS Microbiol. Rev. 27 (2–3), 183–195. http://dx.doi.org/10.1016/S0168-6445(03)00053-6.
Tatusov, R.L., Galperin, M.Y., Natale, D.A., Koonin, E.V., 2000. The COG database: a tool for genome-scale analysis of protein functions and evolution. Nucleic Acids Res. 28, 33–36. http://dx.doi.org/10.1093/nar/28.1.33.
Theilacker, C., Holst, O., Lindner, B., Huebner, J., Kaczyński, Z., 2012. The structure of the wall teichoic acid isolated from *Enterococcus faecalis* strain 12030. Carbohydr. Res. 354, 106–109. http://dx.doi.org/10.1016/j.carres.2012.03.031.
Trapnell, C., Williams, B.a., Pertea, G., Mortazavi, A., Kwan, G., van Baren, M.J., Salzberg, S.L., Wold, B.J., Pachter, L., 2010. Transcript assembly and quantification by RNA-Seq reveals unannotated transcripts and isoform switching during cell differentiation. Nat. Biotechnol. 28, 511–515. http://dx.doi.org/10.1038/nbt.1621.
van der Veen, S., Abee, T., 2011. Bacterial SOS response: a food safety perspective. Curr. Opin. Biotechnol. 22 (2), 136–142. http://dx.doi.org/10.1016/j.copbio.2010.11.012.
Wang, X., Tong, H., Dong, X., 2014. PerR-regulated manganese ion uptake contributes to oxidative stress defense in an oral *Streptococcus*. Appl. Environ. Microbiol. 80, 2351–2359. http://dx.doi.org/10.1128/AEM.00064-14.
Wroblowa, H.S., Yen Chi, P., Razumney, G., 1976. Electroreduction of oxygen: a new mechanistic criterion. J. Electroanal. Chem. Interfacial Electrochem. 69, 195–201. http://dx.doi.org/10.1016/S0022-0728(76)80250-1.
Wunderli-Ye, H., Solioz, M., 1999. Copper homeostasis in *Enterococcus hirae*. Adv. Exp. Med. Biol. 448, 255–264.
Yeager, E., 1984. Electrocatalysts for O_2 reduction. Electrochim. Acta 29, 1527–1537. http://dx.doi.org/10.1016/0013-4686(84)85006-9.
Yoshida, Y., Furuta, S., Niki, E., 1993. Effects of metal chelating agents on the oxidation of lipids induced by copper and iron. Biochim. Biophys. Acta 1210, 81–88.